Biochimica et Biophysica Acta 1853 (2015) 1406–1415

Contents lists available at ScienceDirect

Biochimica et Biophysica Acta

journal homepage: www.elsevier.com/locate/bbamcr

Review

The role of X-ray spectroscopy in understanding the geometric and electronic structure of nitrogenase☆

Joanna Kowalska [a], Serena DeBeer [a,b,*]

[a] Max Planck Institute for Chemical Energy Conversion, Stiftstrasse 34-36, D-45470 Mülheim an der Ruhr, Germany
[b] Department of Chemistry and Chemical Biology, Cornell University, Ithaca, NY 14853, USA

ARTICLE INFO

Article history:
Received 15 September 2014
Received in revised form 22 November 2014
Accepted 24 November 2014
Available online 5 December 2014

Keywords:
Nitrogenase
X-ray absorption spectroscopy
XAS
X-ray emission spectroscopy
XES
Electronic structure

ABSTRACT

X-ray absorption (XAS) and X-ray emission spectroscopy (XES) provide element specific probes of the geometric and electronic structures of metalloprotein active sites. As such, these methods have played an integral role in nitrogenase research beginning with the first EXAFS studies on nitrogenase in the late 1970s. Herein, we briefly explain the information that can be extracted from XAS and XES. We then highlight the recent applications of these methods in nitrogenase research. The influence of X-ray spectroscopy on our current understanding of the atomic structure and electronic structure of iron molybdenum cofactor (FeMoco) is emphasized. Contributions of X-ray spectroscopy to understanding substrate interactions and cluster biosynthesis are also discussed. This article is part of a Special Issue entitled: Fe/S proteins: Analysis, structure, function, biogenesis and diseases.

1. Introduction

Nearly 80% of the earth's atmosphere is comprised of inert dinitrogen (N_2), which must be converted into a bioavailable form for incorporation into both amino and nucleic acids, the building blocks of proteins and DNA. Industrially, the conversion of dinitrogen to ammonia is achieved using heterogeneous catalysts in the well-known Haber–Bosch process, which operates at high temperatures and pressures. The Haber–Bosch process is utilized to produce fertilizers and as such is often credited for the dramatic increase in the global population, which followed its discovery. Prior to the invention of the Haber–Bosch process, nitrogenase enzymes, found in bacteria and free diazotrophs, provided the dominant (~95%) source of fixed bioavailable nitrogen (with the remaining ~5% deriving from atmospheric N_2 conversion).

The nitrogenase family of enzymes includes Mo-dependent, V-dependent and Fe-dependent forms, all of which can affect the reduction of dinitrogen (N_2) to ammonia (NH_3) under ambient conditions. By far the best studied nitrogenase enzymes are the Modependent forms which utilize eight electrons, eight protons and sixteen ATP molecules in order to produce two molecules of ammonia and one molecule of hydrogen, as shown in the reaction below [1].

$$N_2 + 8H^+ + 8e^- + 16ATP + 16H_2O \rightarrow 2NH_3 + H_2 + 16ADP + 16P_i$$

Mo-dependent nitrogenases consist of two component proteins: the iron protein (which serves as a reductase) and the Mo–Fe protein. The Fe protein is an α_2 homodimer that contains a single [4Fe–4S] cluster that bridges the 2 units. This protein is known as a redox-active agent that is capable of transferring electrons to the MoFe protein. The MoFe protein is an $\alpha_2\beta_2$ heterodimer, where each $\alpha\beta$ unit contains two unique metalloclusters: the P-cluster and the FeMo cofactor (FeMoco) (shown in Fig. 1). The P-cluster is an [8Fe–7S] distorted dicubane, which can be thought of as a [4Fe–4S] cluster and a [4Fe–3S] cluster bridged by sulfides. The P-cluster mediates electron transfer from the [4Fe–4S] cluster of Fe protein to FeMoco. The FeMo cofactor (FeMoco) is a Mo:7Fe:9S:C–homocitrate cluster, which can be viewed as coupled [4Fe–3S] and [Mo–3Fe–3S] clusters. This cofactor is embedded in each α subunit and is generally agreed to be the active site, where substrates bind and are reduced. It is for this reason that particularly strong research efforts have been placed on understanding the structure of the FeMoco cluster [2,3].

X-ray spectroscopy has played an important role in our understanding of nitrogenase cofactors for more than three decades. It was in 1978 that the first Mo EXAFS derived structures of FeMoco were proposed [5,6]. The initial proposals suggested sulfur bridged clusters with either a

☆ This article is part of a Special Issue entitled: Fe/S proteins: Analysis, structure, function, biogenesis and diseases.

* Corresponding author at: Max-Planck-Institut fuer Chemische Energiekonversion Stiftstr. 34-36 Germany. Tel no.: +49 208 306 3605.
E-mail address: serena.debeer@cec.mpg.de (S. DeBeer).

http://dx.doi.org/10.1016/j.bbamcr.2014.11.027

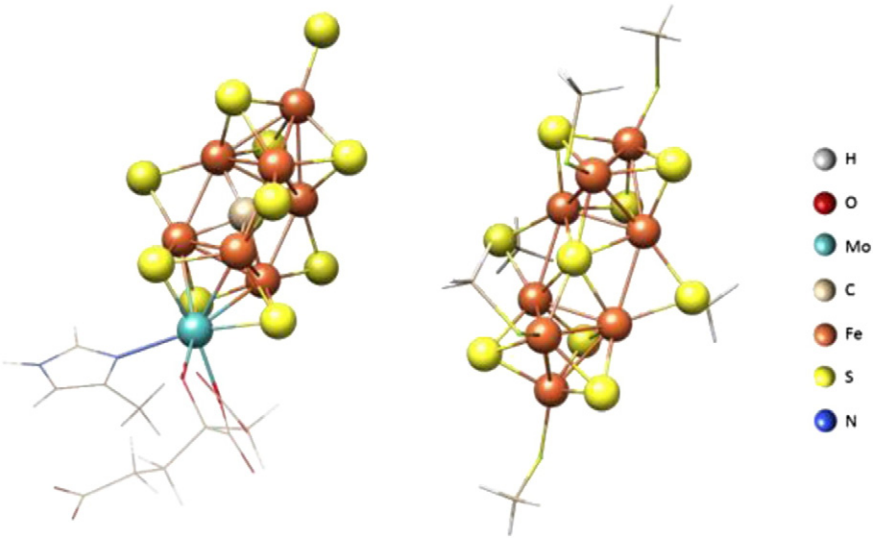

Fig. 1. Structures of the two metalloclusters of nitrogenase: FeMoco (left) and P-cluster (right) (based on PDB: 3U7Q [4]).

linear Fe–Mo–Fe unit or a $MoFe_3$ cubane-like structure. In 1982, the EXAFS proposals were somewhat modified when available Fe EXAFS data suggested that the FeMoco cluster must be larger than simply a single cubane unit [7]. While ultimately the 1992 crystal structure deviated from these initial EXAFS proposals, many of the important structural aspects had already been captured by these early X-ray spectroscopic data — namely, the ~2.35 Å Mo–S and Fe–S distances, as well as the ~2.7 Å Mo–Fe and Fe–Fe distances [5,8]. In the decades that have followed, X-ray spectroscopic methods have continued to play an important role in our understanding of nitrogenase.

In this review, we first give an overview of X-ray spectroscopic methods and the information that can be obtained. We then highlight recent applications of these methods in nitrogenase research.

2. X-ray spectroscopy.

X-ray spectroscopic methods provide element selective probes of electronic and geometric structures. X-ray absorption spectroscopy (XAS) provides information about the unoccupied levels, while X-ray emission spectroscopy (XES) probes the filled levels. Together these two experimental methods can provide a detailed experimental map of the molecular orbitals, giving insight into the oxidation state, spin state, and ligand environment around a specific absorbing atom [9]. In the case of nitrogenase, X-ray spectroscopic studies have allowed all the Fe, Mo and S atoms to be separately probed.

2.1. X-ray absorption spectroscopy (XAS)

X-ray absorption spectroscopy measures the absorption of X-rays as a function of the energy of the incident X-ray. In an XAS spectrum, a dramatic change in the absorption coefficient occurs upon excitation of a core electron. This sharp discontinuity in the spectrum is referred to as an absorption edge. An edge occurs anytime a core electron absorbs an X-ray with energy equal to or greater than its binding energy. The nomenclature of XAS edges reflects the core level from which the electron originates. For example: a K-edge corresponds to the transition from a 1s core orbital, L-edges correspond to 2s and 2p levels, and M-edges to 3s, 3p and 3d levels as shown in Fig. 2 [10]. In the case of nitrogenase research, Fe K- and Mo K-edge XAS have been most extensively applied. However, reports of Mo L- and S K-edge data have also been made [11,12,51].

The resultant XAS spectrum can be divided into two regions:

a) the X-ray absorption near edge structure (XANES) — the low-energy part below, at, and just above (20–50 eV) the edge,

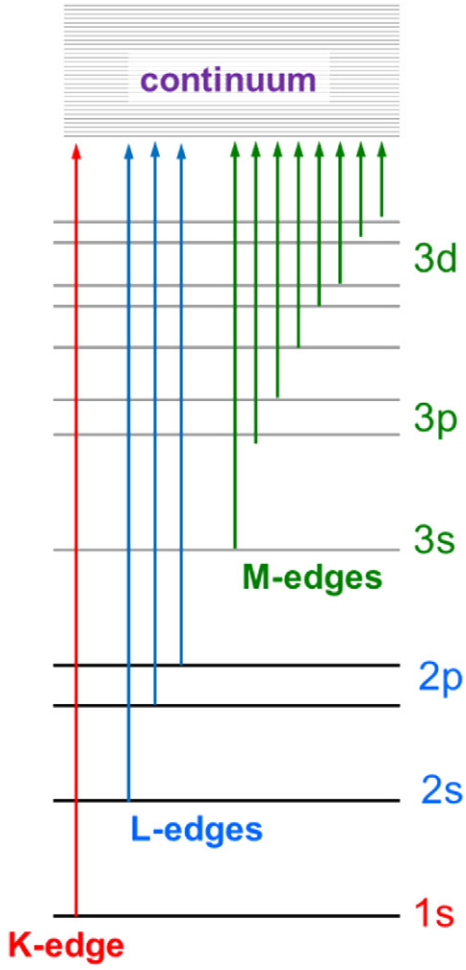

Fig. 2. Transitions resulting from the excitation of a core electron and the corresponding XAS edges.

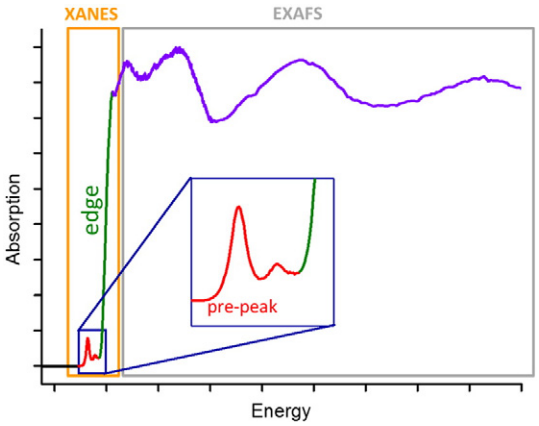

Fig. 3. X-ray absorption spectrum showing the X-ray absorption region near edge structure (XANES) including the pre-edge feature and extended X-ray absorption fine structure (EXAFS) region. Note, in some cases the high energy pre-edge peak may be attributed to charge transfer processes [13].

b) the extended X-ray absorption fine structure (EXAFS) — the higher energy part, tens to hundreds of eV above the edge (Fig. 3).

2.1.1. The X-ray absorption near edge structure (XANES) region

The XANES region shows two characterized features: the already mentioned sharp increase in absorption, which results from the ionization of a core electron and the pre-edge peak, which originates from the transitions to empty molecular orbitals localized on the photoabsorber. The XANES region provides electronic structure information. For first row transition metals the K-edge results from electric dipole allowed 1s to 4p transitions, while the two orders of magnitude lower pre-peak arises from the quadrupole allowed 1s to 3d transitions (Fig. 4).

The position of the edge is usually used as an indicator of the oxidation state of the absorbing atom: the higher the effective charge of an absorbing atom, the more energy that is required to ionize a core electron, resulting in a shift of the edge to higher energies. Typically an increase in 1 unit of oxidation state will result in a ~1–2 eV shift in the edge for compounds with similar ligation environments. We emphasize that it is important to compare systematic series of model complexes, for which the variations in geometric and electronic structural parameters are known, in order to correlate the observed spectral changes with oxidation state trends. As an illustrative example, Fig. 5 shows a comparison of oxidized (Fe(III)Fe(III)) and one-electron reduced (Fe(II)Fe(III)) ferredoxin [14]. In this example, the average Fe oxidation state has changed by 0.5 units, and the edge has shifted by ~0.8 eV. This reference is useful for understanding oxidation state assignments in FeMoco, vide infra.

In addition, the pre-edge features are sensitive to the symmetry of the system. In centrosymmetric transition metal complexes metal 3d and 4p orbitals cannot mix and hence the pre-edge intensities are weak, representing less than 5% of the edge intensity. In contrast, in tetrahedral systems 3d and 4p orbitals mix by symmetry, allowing for the pre-edge to gain intensity due to dipole allowed contributions. We note that for most iron sulfur clusters, intense pre-edges are generally observed due to the tetrahedral coordination environment. The position and number of the peaks are sensitive to the oxidation state (position/shift of the edge), coordination number, covalency and site symmetry [9,12].

Most of the studies on metals in biological systems are conducted at K-edge, due to ease in performing the experiment, as well as the reduction in beam-induced damage. However, it is worth mentioning that it is also possible to carry out studies at L-edges, which result from the dipole allowed 2p to 3d transitions (for 3d metals) (see Fig. 2). In comparison to the K-edge, the L-edge spectra provide 3–5 times better energy resolution resulting in sharper spectrum features [15]. In nitrogenase research, Mo L-edge spectroscopy has been previously applied [11,51]. However, to date Fe L-edge measurements on nitrogenase have not been reported. An alternative method for obtaining higher resolution XAS data is to use high-energy resolution fluorescence detection (HERFD) methods, as highlighted briefly in Section 3.1.2 [16,17].

2.1.2. The extended X-ray absorption fine structure (EXAFS) region

After a core electron has been ionized to the continuum, it can be approximated as a photoelectron wave, which propagates out from the absorbing atom and is backscattered by the electrons of neighboring atoms. The outgoing wave and the backscattered waves will result in interference effects, which result in a modulation of the absorption coefficient, referred to as the extended X-ray absorption fine structure or EXAFS (Fig. 3). Through the analysis of the EXAFS region, information

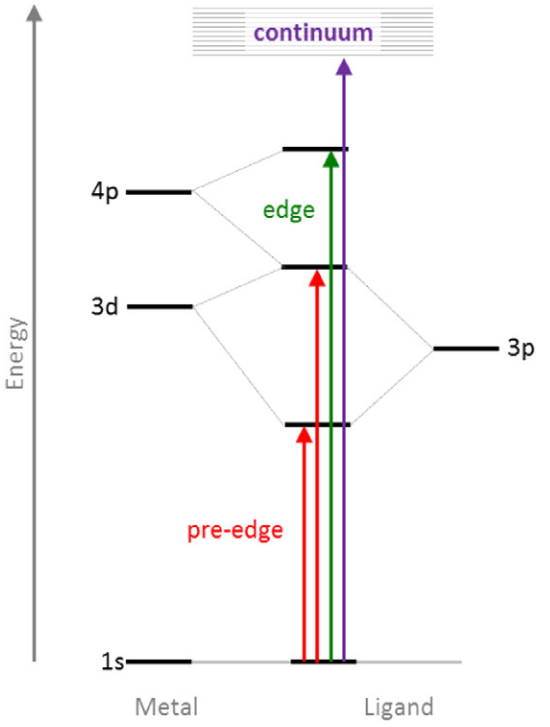

Fig. 4. Energy diagram showing the origin of the K-edge and pre-peak features in X-ray absorption spectrum of transition metals.

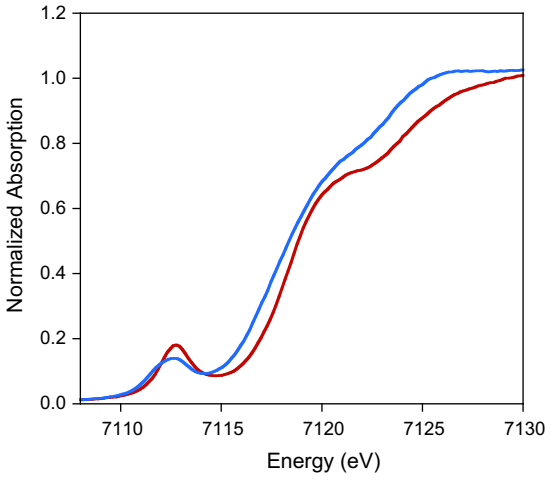

Fig. 5. Comparison of the normalized Fe K-edges for oxidized (red) and reduced ferredoxin (blue).

about the type and distance of the nearest neighboring atoms, can be obtained. In certain cases the bond angle information can also be extracted [18,19]. EXAFS played a particularly important historical role in nitrogenase research. As also noted in the Introduction, the first proposed structures for the FeMoco core were based on EXAFS analysis. Although the exact core structure later proved to be quite different, the Fe–S and Fe–Fe distances were very accurate and provided very important early clues for the complexity of the cluster topology. These EXAFS studies also inspired numerous efforts to synthesize small molecule analogues [20–23].

2.2. X-ray emission spectroscopy (XES)

X-ray emission spectroscopy (XES) is directly related to XAS, as it is a consequence of the absorption of a photon by a core electron. In XES, the core hole created in the X-ray absorption process is immediately ($t \sim 10^{-15}$ s) filled by an electron from a higher level with a subsequent emission of an X-ray photon. The resulting emission processes are labeled as shown in Fig. 6.

The most studied emission lines are the K lines that result from the filling of a 1s orbital hole. The origin of the Kα and Kβ features is shown in Fig. 7 while the complete K emission line spectrum in Fig. 8 [9,24].

2.2.1. The Kα region

The lowest energy emission lines are the Kα lines, which result from the fluorescence which occurs after a 2p electron refills a 1s core hole. Due to 2p spin–orbit coupling, the Kα line will split into two features, the $K\alpha_1$ and $K\alpha_2$ lines. These lines provide little direct chemical information, however, detection of fluorescence data from the Kα line, using a Bragg optic, can be used to obtain XAS data which has resolution dominated not by the 1s core hole lifetime, but rather by the 2p core hole lifetime. These experiments are termed high-energy resolution fluorescence detection (HERFD) [9,17] and can result in an ~5-fold improvement in experimental energy resolution. This methodology was recently applied to obtain higher resolution Mo K-edge data, as described in Section 3.1.2.

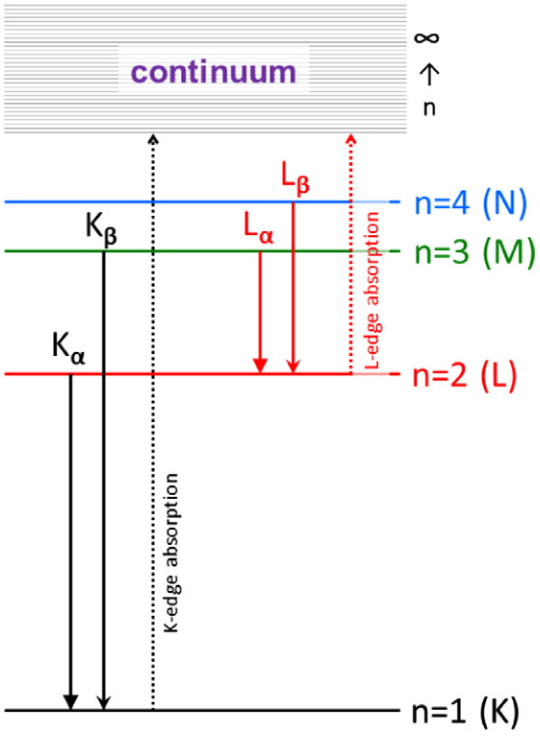

Fig. 6. X-ray emission lines (solid arrows) following the excitation of an electron from the K and L levels. Dashed arrows correspond to ionization of a core electron.

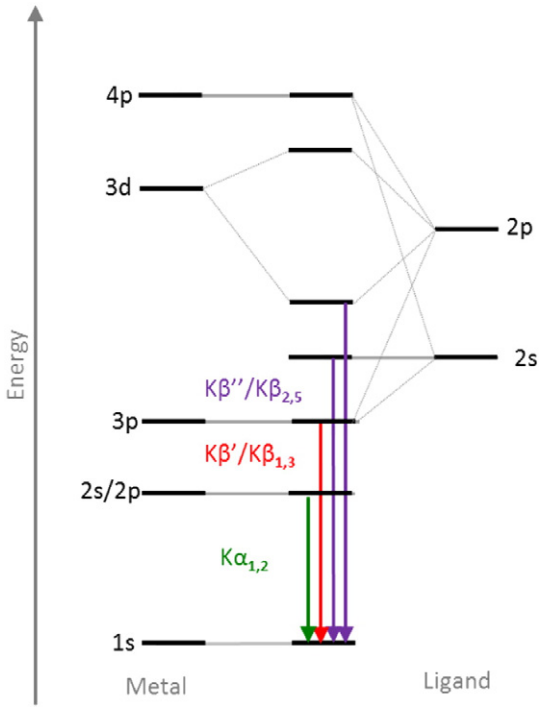

Fig. 7. Energy level diagram for K emission line showing the origin of the Kα and Kβ fine structure.

2.2.2. The Kβ region

The Kβ lines arise from the fluorescence that occurs when 3p (or higher level) electrons refill the 1s core hole. Due to 3p–3d exchange interactions, the main Kβ line can split into $K\beta_{1,3}$ and Kβ′ spectral features. In a simple picture, the greater the number of unpaired electrons, the larger the splitting of the $K\beta_{1,3}$ and Kβ′ features, allowing this spectral region to be used as a marker for spin state [24]. However, recent studies have shown that this simple picture is further complicated by covalent contributions [25]. Furthermore, there is a very low probability (~1000 times less likely than the Kα emission) that a valence electron will refill the 1 s core hole. This gives rise to the $K\beta_{2,5}$ (ligand np to metal 1s) and Kβ″ (ligand ns to metal 1s) transitions, which are collectively referred to as the valence-to-core region or VtC XES. The VtC region provides a sensitive probe of ligand identity, ligand ionization potential and protonation states [26]. This spectral

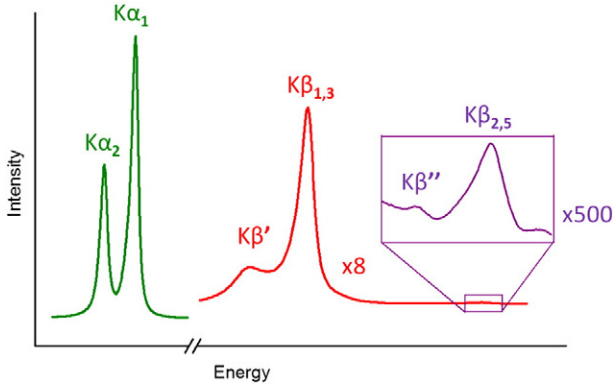

Fig. 8. X-ray emission spectrum showing fine structure of the K lines. Note that Kα lines intensities are ~8 times more intense than the Kβ′ and $K\beta_{1,3}$ features, and ~1000 times more intense than the Kβ″ and $K\beta_{2,5}$ features.

region was particularly important in establishing the presence of a central carbon in FeMoco, as will be highlighted in Section 3.1.1.

A summary of the information that can be obtained from X-ray spectroscopy related to bioinorganic systems is summarized in Fig. 9.

In the last few decades, X-ray spectroscopic methods have undeniably had a large impact on bioinorganic chemistry, and in particular on nitrogenase research. The history begins with the pioneering application of XANES and EXAFS to the MoFe protein by Cramer and Hodgson in the late 1970s [27]. In the years that followed their early EXAFS work [5,6], XAS continued to play a key role in understanding the electronic structure, metrical details and assembly of the active site cofactors. In more recent years, the availability of dedicated beam lines for XES measurements has allowed for the application of VtC XES and HERFD XAS to nitrogenase. Herein, the most recent applications of these X-ray spectroscopic methods and their impact on nitrogenase research are briefly reviewed; this includes basic structural insights, understanding of possible substrate interactions and biosynthesis.

3. Recent applications of X-ray spectroscopy in nitrogenase research

3.1. Structural insights into nitrogenase clusters

3.1.1. The identification of a central carbide in FeMoco

In 2002, Einsle and co-workers first revealed the presence of a central atom in the middle of the FeMoco cluster that could be assigned as a single carbon, nitrogen or oxygen atom [28]. However, due to the resolution of the crystal structure at the time and the challenges associated with identifying light atoms in the presence of heavier atoms (such as Fe, S and Mo) a definitive assignment could not be made. EXAFS studies were utilized by Corbett et al. [29], however their results could not confirm the presence or absence of a light atom. In a separate EXAFS study, George and co-workers combined EXAFS and nuclear resonant vibrational spectroscopy (NRVS) to investigate the identity of the central atom [50,30]. Their results were consistent with the presence of a central atom, but also could not identify it. It was clear that greater selectivity for the ionization potential of ligand was required, and Lancaster et al. achieved this in 2011 by using iron VtC XES. Fig. 10 shows the VtC XES data for the MoFe protein (which contains both the FeMoco cluster and the eight-iron P-cluster),

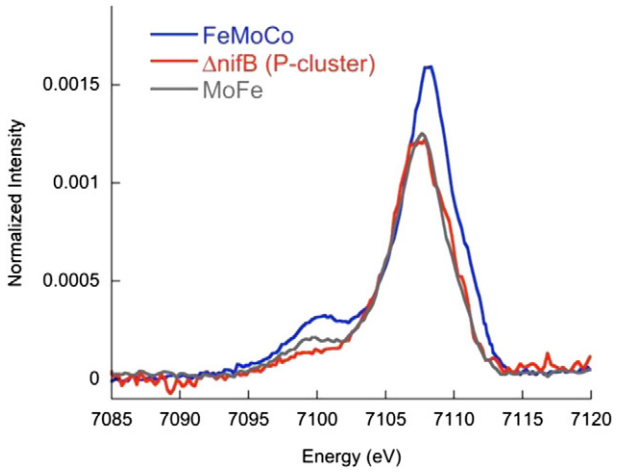

Fig. 10. The experimental V2C XES spectra for isolated FeMoco, MoFe protein, and delta-nifB.
Adapted from Ref. [31]. Copyright 2011 America Association for the Advancement of Science.

the data for isolated FeMoco in N-methyl formamide (NMF), and the data for the delta-NifB gene deletion mutant, which contains only the P-cluster [31]. These experimental data established that only when the FeMoco active site is present that there is a significant intensity at 7101 eV. By correlation of the protein data to model complexes of known coordination environment, the Kβ″ feature was empirically assigned as a carbide. We note that detailed model studies of small molecule complexes of known structures were essential for making this correlation [32–34]. DFT calculations on the FeMoco with different central atoms (i.e. C, N or O) were able to unambiguously assign the central atom as a carbon [31]. This finding was also confirmed by a higher resolution crystal structure and 13C-ESEEM data [35].

3.1.2. Oxidation state distributions in FeMoco

With the identity of the central carbon established, recent efforts have turned to understanding the oxidation state distribution within FeMoco. In general, the following total charge and oxidation state

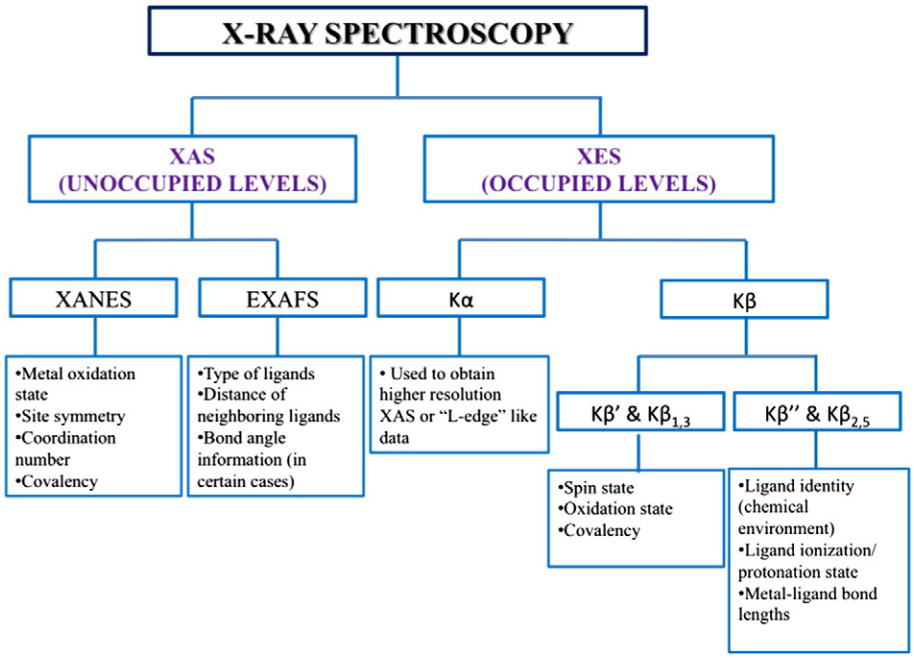

Fig. 9. Summary of information that can be obtained from X-ray spectroscopy.

distributions have been assumed in the literature, all being consistent with an S = 3/2 ground state: 1) $[MoFe_7S_9C]^{1+}$:5 Fe(III):2Fe(II):Mo(IV), 2) $[MoFe_7S_9C]^{1-}$:3Fe(III):4Fe(II):Mo(IV), or 3) $[MoFe_7S_9C]^{3-}$: Fe(III):6Fe(II):Mo(IV). We note, however, that the Mo(IV) oxidation state assignment has recently been reassigned as Mo(III) (vide infra), thus requiring a greater complement of oxidized iron for each of the three possibilities, i.e. $[MoFe_7S_9C]^{1+}$:6Fe(III):1Fe(II):Mo(III), $[MoFe_7S_9C]^{1-}$:4Fe(III):3Fe(II):Mo(III) or $[MoFe_7S_9C]^{3-}$: 2Fe(III):5Fe(II):Mo(III) [36]. As knowledge of the electronic structure is fundamental to any informed mechanistic discussion, efforts have focused on experimentally differentiating between these three possibilities.

Using X-ray spectroscopy to study the Fe oxidation state distribution is intrinsically challenging due to the large number of irons in the MoFe protein (8 Fe atoms in the P-cluster and an additional 7 Fe atoms in FeMoco). Hence, while many Fe XANES studies have been carried out, a clear assignment has yet to be made and even qualitative discussions of the relative oxidation state changes between FeMoco and the P-clusters are relatively scarce. The most detailed studies in this respect are those performed by Corbett et al., who reported the Fe K-edge data for delta NifB (containing only the P-cluster in an all ferrous form), MoFe protein, and "MoFe bound protein FeMoco", which was obtained by subtraction [37]. A comparison of these spectra is shown in Fig. 11 (top panel). Interestingly, the rising edge inflection points for the P-cluster and MoFe protein bound FeMoco overlay, seemingly suggesting that FeMoco has a relatively small fraction of oxidized iron, such that experimentally no shift in the ~7119 eV rising edge is observed. We note that previous studies of the two electron oxidized P-cluster also showed overlapping edge positions for the P^N (all ferrous) and P^{ox} forms (two electron oxidized), indicating that oxidation of two out of eight irons results in no observable shift in the ~7119 eV rising edge position [38]. In contrast, changes are observed in the intensity of the ~7126 eV feature. The decrease in the ~7126 eV intensity for MoFe bound FeMoco relative to the P-clusters is consistent with the presence of some complement of oxidized Fe. However, the precise extent of this is further complicated by the differences in the local coordination environments in the P-clusters vs. FeMoco, i.e. a local FeS_4 coordination sphere vs. an FeS_3C coordination sphere. These differences in the local coordination environment may also account for the increase in pre-edge intensity for MoFe bound protein FeMoco relative to the P-cluster, as also suggested by Corbett et al. We note that similar comparisons can also be made with isolated FeMoco. Fig. 11 (bottom) shows a comparison of the MoFe bound FeMoco to isolated FeMoco in NMF (as reported by Fay et al. [39]). While the overall edge shapes are very similar, the isolated FeMoco edge appears to ~0.3 eV lower energy. This may be attributed to a perturbation of the FeMoco ligation sphere upon extraction into NMF and/or to slight differences in the experimental calibrations. Nonetheless at this stage, a definitive assignment of the Fe oxidation state based on Fe K-edge XAS remains elusive. It does, however, appear that the $[MoFe_7S_9C]^{1+}$, which requires a large complement of oxidized iron (i.e. 6Fe(III):1Fe(II) and 1 Mo(III)), is unlikely to be consistent with the Fe K-edge data. A more quantitative assessment of these data will require correlations to computational studies and also the measurement of higher resolution XAS data. These studies are currently underway in our laboratories.

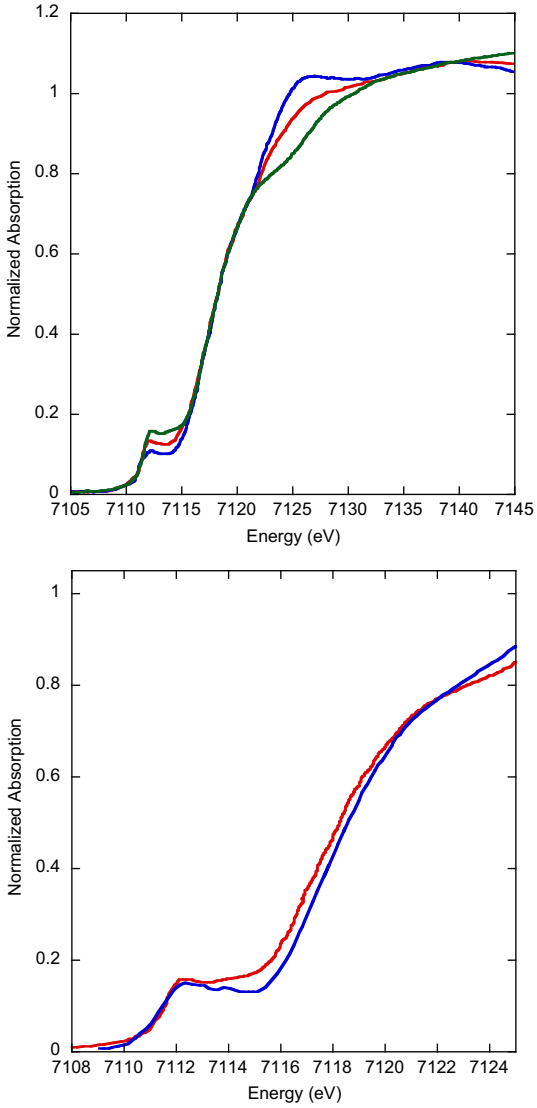

Fig. 11. (top) Normalized Fe K-edge spectra for delta NifB (blue), MoFe protein (red), and MoFe bound FeMoco (green), as reported by Corbett [37] (Copyright (2006) National Academy of Sciences, U.S.A.). (bottom) Comparison of MoFe bound FeMoco (blue) and isolated FeMoco (red) (isolated FeMoco data were reported by Fay et al. [39] Copyright © 2011 WILEY-VCH Verlag GmbH & Co. KGaA).

While the Fe oxidation state assignment remains uncertain, progress has been made in understanding the electronic structure of Mo and its coupling into the FeMoco cluster. Based primarily on Mo-95 ENDOR studies in the 1980s, a Mo(IV) assignment has generally been assumed for FeMoco [40]. It is interesting to note that early XAS studies by Hodgson and coworkers had very cautiously assigned the Mo oxidation state as either Mo(III) or Mo(IV) based on Mo–S distances, and only later was the XAS assignment revised [11] in order to be consistent with ENDOR studies. Of course, as first noted by Hodgson et al., one of the main challenges in using XAS to assign the oxidation state assignments from the Mo K-edge is the large core hole lifetime broadening at Mo, which renders the edges rather featureless. In order to address this issue, we have recently utilized HERFD XAS to obtain higher resolution data at the Mo K-edge [16]. By comparison to model complexes of known oxidation states, we were able to definitively assign the Mo oxidation state assignment as Mo(III) [36]. Of particular importance was the comparison of MoFe protein to data on MoFe model complexes with Mo(III) and Mo(V) oxidation states. For this purpose data were obtained on $[Cl_2Fe(III)(\mu\text{-}S)_2Mo(V)(O)_3(Cl_4Cat)]^{2-}$ [21] and $[(Tp)Mo(III)Fe(II,III,III)_3S_4Cl_3]^{1-}$ [22], previously reported by Coucouvanis and Holm, respectively. For reference, the structures are shown in Fig. 12, and the corresponding Mo HERFD XAS data are shown in Fig. 13. The Mo(V)Fe dimer has a rising edge that clearly appears at higher energy, consistent with an increase in oxidation state by 2 units relative to the Mo(III)Fe3 cubane. If a Mo(IV) assignment were appropriate for MoFe protein, it should have a rising edge that falls between the two model complexes. However, MoFe protein appears if anything to slightly lower energy, thus ruling out a Mo(IV) assignment and providing stronger support for Mo(III). This assignment was further verified by time dependent DFT calculations of both the model complexes and FeMoco. Further, through DFT calculations, we were able to show that the Mo has a d^3 configuration with an unusual

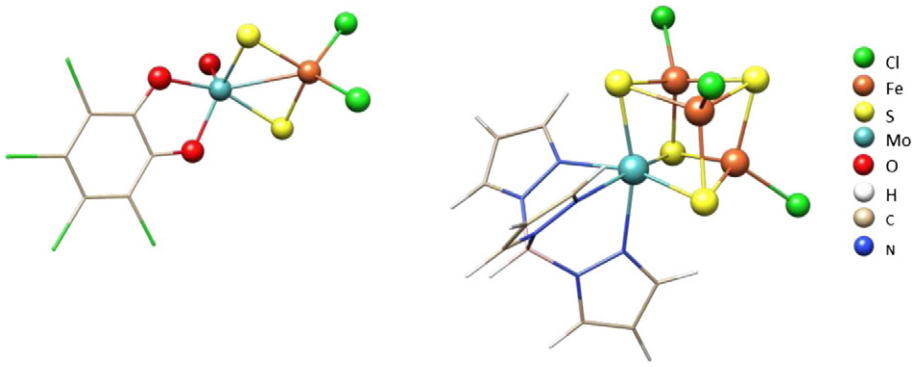

Fig. 12. Structures of FeMo model compounds used in the study to assign the Mo oxidation state in FeMoco: $[Cl_2Fe(III)(u\text{-}S)_2\ Mo(V)(O)_3\ (Cl_4Cat)]^{2-}$ [19] (left) and $[(Tp)Mo(III)Fe(II,III,III)_3S_4Cl_3]^{1-}$ [20] (right).

"non-Hund" alpha-beta-beta low spin configuration, which may be attributed to spin coupling with the Fe atoms [36]. Whether this unusual Mo spin configuration truly represents an excited spin state of the molybdenum or whether the configuration arises due to spin-canting effects in the cubane system, remains an open question. In any case, this assignment requires a reassessment of the Fe oxidation state distribution as noted above.

While the majority of X-ray spectroscopic studies have focused on Mo-dependent nitrogenases, there has also been recent progress on studies of vanadium-dependent nitrogenases by the collaborative groups of Ribbe and Hodgson. The differences between Mo- and V-dependent nitrogenases are of particular interest as the latter has been shown to effectively catalyze C – C bond formation [41]. Hence, one would like to know what the electronic structural differences are that mediate these differences in reactivity. The earliest XAS studies on vanadium nitrogenase were carried out by Arber et al. in 1987 [42]. In this study, V K-edge XAS data were reported for vanadium nitrogenase from *Azotobacter chroococcum* and compared to a $[VFe_3S_4Cl_3(DMF)_3]$ model complex, synthesized by Holm and co-workers. Based on this comparison the authors concluded that the vanadium site was in a distorted octahedral environment with an oxidation state somewhere between V(II) and V(IV). In 1988, George and co-workers reported similar results on vanadium nitrogenase from *Azotobacter vinelandii* [43]. In addition, their work established an elongation of the M–Fe distances in V nitrogenases relative to Mo nitrogenases, which they indicated could relate to differences in observed reactivity. Interestingly, there have been no further reports of V XAS data on VFe. However, in 2010 Fay et al. reported Fe K-edge XAS data on FeVco in comparison to isolated FeMoco [44]. Their results showed clear differences in the rising edge and pre-edge regions of the two clusters (Fig. 14, panels A and B), with the FeVco data shifted almost ~2 eV to higher energy than FeMoco. The authors indicate that this may be attributed to differences in the Fe coordination environment in FeMoco vs. FeVco, with the latter having a greater complement of light atom contributions based on EXAFS analysis (Fig. 14, panels C and D). The authors' interpretation of this result is that FeVco is surrounded by a well-ordered sphere of NMF, while in FeMoco there are either fewer and/or more disordered interactions with solvent. Based on these data, it is also argued that the FeVco cofactor is more elongated than FeMoco consistent with the 1988 report of George et al. [43]. However, it should be noted that the Blank et al. Fe–Fe and Fe–V distances in FeVco are substantially longer than those initially reported by George et al. on intact VFe protein (2.88 Å vs 2.75 Å), and could suggest that the extracted FeVco preparation may have been partially compromised. In any case, the differences in the electronic and geometric structures of FeMoco and FeVco is clearly an area of great interest and one which warrants further investigation.

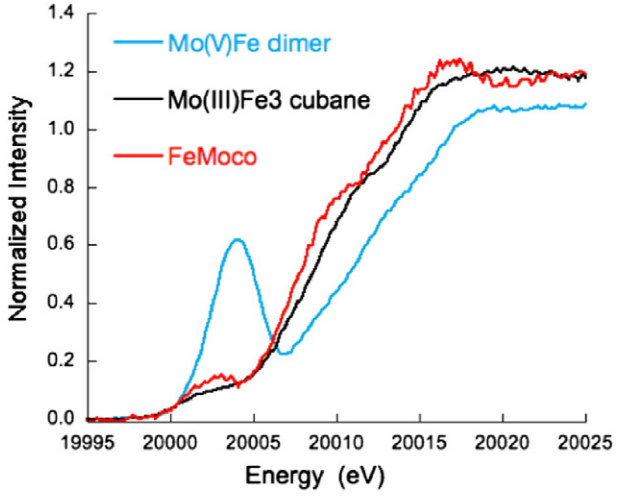

Fig. 13. Normalized Mo HERFD XAS data for FeMo compounds: $[Cl_2Fe(III)(u\text{-}S)_2\ Mo(V)(O)_3\ (Cl_4Cat)]^{2-}$ (Mo(V)Fe dimer [21]) and $[(Tp)Mo(III)Fe(II,III,III)_3S_4Cl_3]^{1-}$ (Mo(III)Fe3 cubane [22]) and FeMoco.
Adapted from Ref. [36] with permission from the Royal Society of Chemistry (2014).

3.2. Interaction of FeMoco with substrate

Toward the goal of understanding how nitrogenase reduces the triple bond of dinitrogen, one would ultimately like to use X-ray spectroscopy to examine the interaction of substrate, and its transformation to ammonia. This, however, presents many intrinsic challenges. The MoFe protein requires the presence of its native reductase (the Fe protein) in order to turn over, thus further limiting any selectivity at the Fe K-edge. In addition, there are inherent obstacles in synchronizing the electron delivery to the MoFe protein, thus inhibiting the ability to generate specific intermediates. In order to overcome these challenges, the groups of Dean and Seefelt have made point mutations near the FeMoco active site to allow for the interaction of larger substrates, such as propargyl alcohol, which can then be trapped and studied as potential substrate analogues for N_2. One recent study by Cramer, Sean, Seefeldt and coworkers used a combination of NRVS and Fe/Mo K-edge XAS to study the alph-70^{Ala} variant of *A. vinelandii* [45]. Based on these data, the authors suggested that propargyl alcohol (PA) binds to the Fe6 or Fe7 iron atoms adjacent to the Mo, as shown in Fig. 15. In our view, however, the changes in the XAS data are rather subtle, and it is difficult to state that these data provide unambiguous evidence for the interaction of PA with Fe. It is clear that the need for greater selectivity for specific Fe–substrate interactions remains one of the challenges and limitations of X-ray spectroscopic approaches.

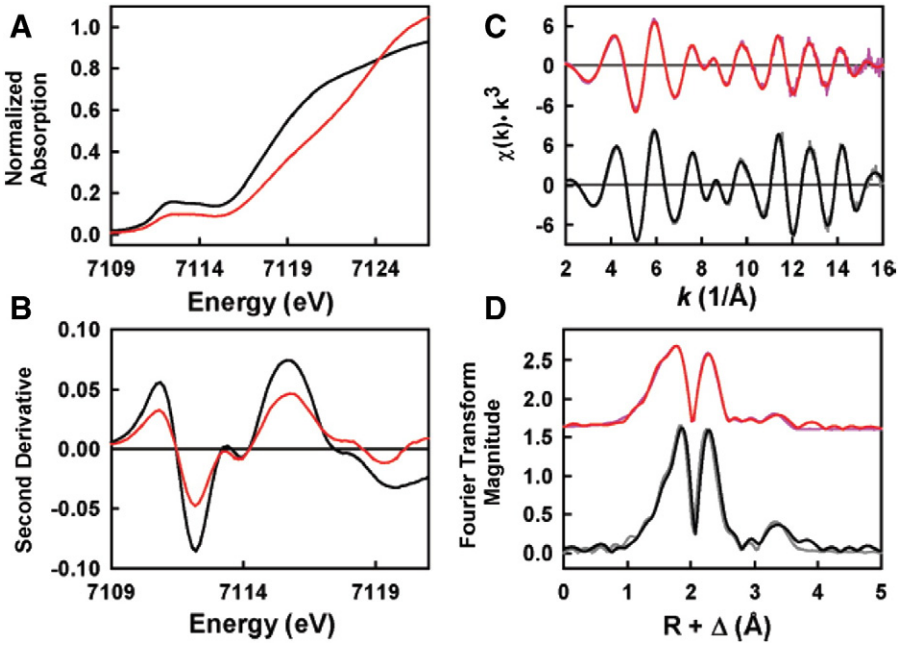

Fig. 14. (A) Fe K-edge XAS spectra and (B) second derivatives for NMF-extracted FeVco (red) and FeMoco (black). (C) Fe K-edge EXAFS and (D) Fourier transforms of data (red) and fits (red) for FeVco, and those of data (gray) and fits (black) for FeMoco.
Adapted from Ref. [44] with permission from ACS Publications.

3.3. Biosynthesis

In addition to providing insights into the electronic structure and the interactions of substrate with cofactor, X-ray spectroscopy has also provided valuable information regarding the biosynthesis of FeMoco. It is well known that the assembly of FeMoco begins with the formation of Fe_2S_2 and Fe_4S_4 fragments of NifS and NifU, respectively [46]. These smaller fragments are then assembled on NifB and further matured on NifEN. Based on initial EXAFS studies, it was suggested that the "L-cluster" of NifEN was either a 7 or 8 iron core. Subsequent EXAFS measurements on the isolated L-cluster showed that the L-cluster was best described as an 8 iron core, with either contributions from central light atoms and/or solvent contributions [29]. In 2013, VtC XES studies, established that the L-cluster in fact contains a central carbon, thus providing experimental evidence that carbon insertion occurs on NifB [47]. This was also elegantly demonstrated by Ribbe and coworkers by using 14-C labeling of s-adenosyl methionine to show that a methyl group was the source of the central carbon atom [48].

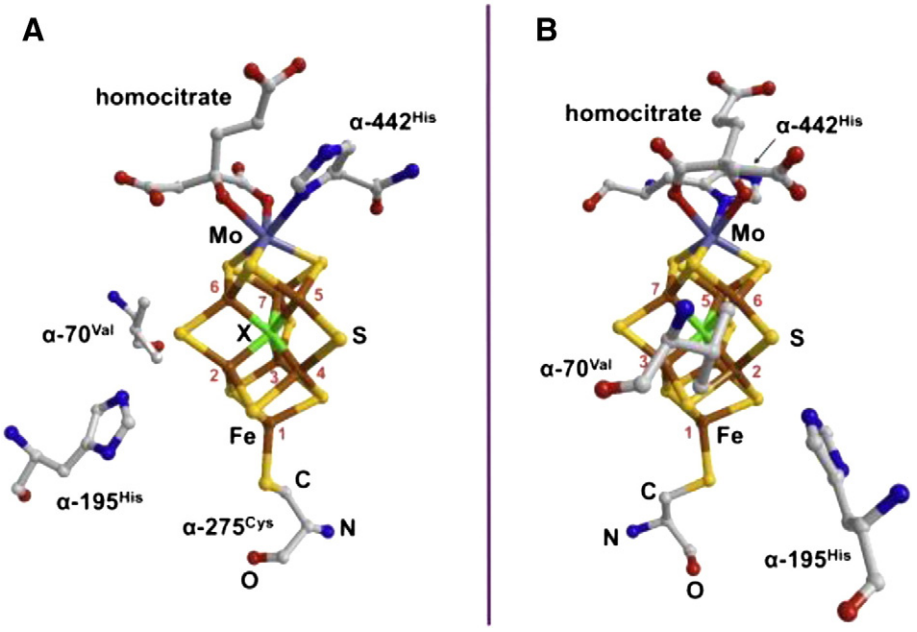

Fig. 15. The structure of the FeMoco (PRB: 1M1N). Mo — purple, Fe — brown, S — yellow, O — red, N — blue, C — gray, X — gray. The Fe atoms are numbered in red.
Adapted from Ref. [45] with permission from Elsevier.

4. Summary and outlook

Herein, we have briefly reviewed recent contributions of X-ray spectroscopy to our present understanding of nitrogenase. The last several years have seen the identification of a central carbon by XES, the assignment of a Mo(III) in the ground state of FeMoco based on HERFD XAS, and evidence for substrate interactions at Fe from both EXAFS and NRVS. XAS and XES have also both provided fundamental insights into cofactor biosynthesis.

However, it is clear that numerous open questions remain. The charge of the FeMoco is still not definitively assigned, and in particular, many open questions remain about the differences between FeVco and FeMoco. It is here that high-resolution X-ray spectroscopic measurements, such as the HERFD XAS measurements utilized at Mo, may provide a more quantitative understanding of the electronic structure changes. In our view, the continued close coupling of experiment and theory will play an essential role. The identification of substrate interactions will likely continue to pose a major challenge. However, the recent reports of ligand selective XAS, gives promise that two-dimensional X-ray spectroscopic approaches may enable the identification of specific metal substrate interactions [49].

Acknowledgements

JK and SD acknowledge the Max Planck Society for funding. SD acknowledges funding from the European Research Council under the European Union's Seventh Framework Programme (FP/2007–2013) ERC Grant Agreement No. 615414.

References

[1] B.E. Smith, Nitrogenase reveals its inner secrets, Science 297 (2002) 1654–1655.
[2] B.M. Hoffman, D. Lukoyanov, Z.Y. Yang, D.R. Dean, L.C. Seefeldt, Mechanism of nitrogen fixation by nitrogenase: the next stage, Chem. Rev. 114 (2014) 4041–4062.
[3] M.W. Ribbe, Y.L. Hu, K.O. Hodgson, B. Hedman, Biosynthesis of nitrogenase metalloclusters, Chem. Rev. 114 (2014) 4063–4080.
[4] http://www.rcsb.org/pdb/explore/literature.do?structureId=3U7Q&bionumber=1PDB:3U7Q.
[5] S.P. Cramer, K.O. Hodgson, W.O. Gillum, L.E. Mortenson, Molybdenum site of nitrogenase — preliminary structural evidence from X-ray absorption spectroscopy, J. Am. Chem. Soc. 100 (1978) 3398–3407.
[6] S.P. Cramer, W.O. Gillum, K.O. Hodgson, L.E. Mortenson, E.I. Stiefel, J.R. Chisnell, W.J. Brill, V.K. Shah, Molybdenum site of nitrogenase. 2. Comparative-study of Mo–Fe proteins and iron–molybdenum cofactor by X-ray absorption spectroscopy, J. Am. Chem. Soc. 100 (1978) 3814–3819.
[7] M.R. Antonio, B.K. Teo, W.H. Ormejohnson, M.J. Nelson, S.E. Groh, P.A. Lindahl, S.M. Kauzlarich, B.A. Averill, Iron EXAFS of molybdenum cofactor of nitrogenase, J. Am. Chem. Soc. 104 (1982) 4703–4705.
[8] J.S. Kim, D.C. Rees, Structural models for the metal centers in the nitrogenase molybdenum–iron protein, Science 257 (1992) 1677–1682.
[9] J. Sa (Ed.), High-resol ution XAS/XES: Analyzing Electronic Structure of Catalysts, Taylor & Francis Group, LLC2014.
[10] C. Bressler, M. Chergui, Ultrafast X-ray absorption spectroscopy, Chem. Rev. 104 (2004) 1781–1812.
[11] B. Hedman, P. Frank, S.F. Gheller, A.L. Roe, W.E. Newton, K.O. Hodgson, New structural insights into the iron molybdenum cofactor from *Azotobacter vinelandii* nitrogenase through sulfur–K and molybdenum–L X-ray absorption-edge studies, J. Am. Chem. Soc. 110 (1988) 3798–3805.
[12] C.J. Pollock, L.L. Tan, W. Zhang, K.M. Lancaster, S.C. Lee, S. DeBeer, Light-atom influences on the electronic structures of iron sulfur clusters, Inorg. Chem. 53 (2014) 2591–2597.
[13] M. Roemelt, M.A. Beckwith, C. Duboc, M.N. Collomb, F. Neese, S. DeBeer, Manganese K-edge X-ray absorption spectroscopy as a probe of the metal–ligand interactions in coordination compounds, Inorg. Chem. 51 (2012) 680–687.
[14] S. DeBeer, X-ray absorption spectroscopy, in: Markus W. Ribbe (Ed.), Methods in Molecular Biology, Nitrogen FixationHumana Press (Springer), 2011, pp. 165–176.
[15] F. de Groot, High resolution X-ray emission and X-ray absorption spectroscopy, Chem. Rev. 101 (2001) 1779–1808.
[16] F.A. Lima, R. Bjornsson, T. Weyhermueller, P. Chandrasekaran, P. Glatzel, F. Neese, S. DeBeer, High-resolution molybdenum K-edge X-ray absorption spectroscopy analyzed with time-dependent density functional theory, Phys. Chem. Chem. Phys. 15 (2013) 20911–20920.
[17] K. Hamalainen, D.P. Siddons, J.B. Hastings, L.E. Berman, Elimination of the inner-shell lifetime broadening in X-ray absorption spectroscopy, Phys. Rev. Lett. 67 (1991) 2850–2853.
[18] J.J. Rehr, R.C. Albers, Theoretical approaches to X-ray absorption fine structure, Rev. Mod. Phys. 72 (2000) 621–654.
[19] D.C. Koningsberger, Prins R X-ray Absorption, Principles, Applications Techniques of EXAFS, SEXAFS, and XANES, Wiley, New York, NY, 1998.
[20] R. Bjornsson, F. Neese, R.R. Schrock, O. Einsle, S. DeBeer, The discovery of Mo(III) in FeMoco: reuniting enzyme and model chemistry, J. Biol. Inorg. Chem. (2014) (submitted for publication). http://dx.doi.org/10.1007/s00775-014-1230-6.
[21] D. Coucouvanis, Fe–M–S complexes derives from MS42-Anions (M = Mo, W) and their possible relevance as analogs for structural features in the Mo site of nitrogenase, Acc. Chem. Res. 14 (1981) 201–209.
[22] S.C. Lee, R.H. Holm, The clusters of nitrogenase: synthetic methodology in the construction of weak-field clusters, Chem. Rev. 104 (2004) 1135–1157.
[23] P.V. Rao, R.H. Holm, Synthetic analogues of the active sites of iron–sulfur proteins, Chem. Rev. 104 (2004) 527–559.
[24] P. Glatzel, U. Bergmann, High resolution 1 s core hole X-ray spectroscopy in 3d transition metal complexes — electronic and structural information, Coord. Chem. Rev. 249 (2005) 65–95.
[25] C.J. Pollock, M.U. Delgado-Jaime, M. Atanasov, F. Neese, S. DeBeer, K beta mainline X-ray emission spectroscopy as an experimental probe of metal–ligand covalency, J. Am. Chem. Soc. 136 (2014) 9453–9463.
[26] E. Gallo, P. Glatzel, P Adv. Mater. (2014), http://dx.doi.org/10.1002/adma.201304994.
[27] S.P. Cramer, T.K. Eccles, F.W. Kutzler, K.O. Hodgson, L.E. Mortenson, Molybdenum X-ray absorption-edge spectra — chemical state of molybdenum in nitrogenase, J. Am. Chem. Soc. 98 (1976) 1287–1288.
[28] O. Einsle, F.A. Tezcan, S.L.A. Andrade, B. Schmid, M. Yoshida, J.B. Howard, D.C. Rees, Nitrogenase MoFe-protein at 1.16 angstrom resolution: a central ligand in the FeMo-cofactor, Science 297 (2002) 1696–1700.
[29] M.C. Corbett, Y.L. Hu, F. Naderi, M.W. Ribbe, B. Hedman, K.O. Hodgson, Comparison of iron–molybdenum cofactor-deficient nitrogenase MoFe proteins by X-ray absorption spectroscopy — implications for P-cluster biosynthesis, J. Biol. Chem. 279 (2004) 28276–28282.
[30] S.J. George, R.Y. Igarashi, Y. Xiao, J.A. Hernandez, M. Demuez, D. Zhao, Y. Yoda, P.W. Ludden, L.M. Rubio, S.P. Cramer, Extended X-ray absorption fine structure and nuclear resonance vibrational spectroscopy reveal that NifB-co, a FeMo-co precursor, comprises a 6Fe core with an interstitial light atom, J. Am. Chem. Soc. 130 (2008) 5673–5680.
[31] K.M. Lancaster, M. Roemelt, P. Ettenhuber, Y. Hu, M.W. Ribbe, F. Neese, U. Bergmann, S. DeBeer, X-ray emission spectroscopy evidences a central carbon in the nitrogenase iron–molybdenum cofactor, Science 334 (2011) 974–977.
[32] N. Lee, T. Petrenko, U. Bergmann, F. Neese, S. DeBeer, Probing valence orbital composition with iron K beta X-ray emission spectroscopy, J. Am. Chem. Soc. 132 (2010) 9715–9727.
[33] M.U. Delgado-Jaime, B.R. Dible, K.P. Chiang, W.W. Brennessel, U. Bergmann, P.L. Holland, S. DeBeer, Identification of a single light atom within a multinuclear metal cluster using valence-to-core X-ray emission spectroscopy, Inorg. Chem. 50 (2011) 10709–10717.
[34] P. Chandrasekaran, K.P. Chiang, D. Nordlund, U. Bergmann, P.L. Holland, S. DeBeer, Sensitivity of X-ray core spectroscopy to changes in metal ligation: a systematic study of low-coordinate, high-spin ferrous complexes, Inorg. Chem. 52 (2013) 6286–6298.
[35] T. Spatzal, M. Aksoyoglu, L. Zhang, S.L.A. Andrade, E. Schleicher, S. Weber, D.C. Rees, O. Einsle, Evidence for interstitial carbon in nitrogenase FeMo cofactor, Science 334 (2011) 940.
[36] R. Bjornsson, F.A. Lima, T. Spatzal, T. Weyhermueller, P. Glatzel, E. Bill, O. Einsle, F. Neese, S. DeBeer, Identification of a spin-coupled Mo(III) in the nitrogenase iron–molybdenum cofactor, Chem. Sci. 5 (2014) 3096–3103.
[37] M.C. Corbett, Y.L. Hu, A.W. Fay, M.W. Ribbe, B. Hedman, K.O. Hodgson, Structural insights into a protein-bound iron–molybdenum cofactor precursor, Proc. Natl. Acad. Sci. U. S. A. 103 (2006) 1238–1243.
[38] K.B. Musgrave, H.I. Liu, L. Ma, B.K. Burgess, G. Watt, B. Hedman, K.O. Hodgson, EXAFS studies on the P(N) and P(OX) states of the P-clusters in nitrogenase, J. Biol. Inorg. Chem. 3 (1998) 344–352.
[39] A.W. Fay, M.A. Blank, C.C. Lee, Y. Hu, K.O. Hodgson, B. Hedman, M.W. Ribbe, Spectroscopic characterization of the isolated iron–molybdenum cofactor (FeMoco) precursor from the protein NifEN, Angew. Chem. Int. Ed. 50 (2011) 7787–7790.
[40] R.A. Venters, M.J. Nelson, P.A. McLean, A.E. True, M.A. Levy, B.M. Hoffman, W.H. Ormejohnson, ENDOR of the resting state of nitrogenase molybdenum iron proteins from *Azotobacter vinelandii*, *Klebsiella pneumoniae*, and *Clostridium pasteurianum* — H-1, Fe-57, Mo-95, and S-33 studies, J. Am. Chem. Soc. 108 (1986) 3487–3498.
[41] Y. Hu, C.C. Lee, M.W. Ribbe, Extending the carbon chain: hydrocarbon formation catalyzed by vanadium/molybdenum nitrogenases, Science 333 (2011) 753–755.
[42] J.M. Arber, B.R. Dobson, R.R. Eady, P. Stevens, S.S. Hasnain, C.D. Garner, B.E. Smith, Vanadium K-edge X-ray absorption-spectrum of the VFe protein of the vanadium nitrogenase of *Azotobacter chroococum*, Nature 325 (1987) 372–374.
[43] G.N. George, C.L. Coyle, B.J. Hales, S.P. Cramer, X-ray absorption of *Azotobacter vinelandii* vanadium nitrogenase, J. Am. Chem. Soc. 110 (1988) 4057–4059.
[44] A.W. Fay, M.A. Blank, C.C. Lee, Y. Hu, K.O. Hodgson, B. Hedman, M.W. Ribbe, Characterization of isolated nitrogenase FeVco, J. Am. Chem. Soc. 132 (2010) 12612–12618.
[45] S.J. George, B.M. Barney, D. Mitra, R.Y. Igarashi, Y. Guo, D.R. Dean, S.P. Cramer, L.C. Seefeldt, EXAFS and NRVS reveal a conformational distortion of the FeMo-cofactor in the MoFe nitrogenase propargyl alcohol complex, J. Inorg. Biochem. 112 (2012) 85–92.
[46] G. Schwarz, R.R. Mendel, M.W. Ribbe, Molybdenum cofactors, enzymes and pathways, Nature 460 (2009) 839–847.

[47] K.M. Lancaster, Y. Hu, U. Bergmann, M.W. Ribbe, S. DeBeer, X-ray spectroscopic observation of an interstitial carbide in NifEN-bound FeMoco precursor, J. Am. Chem. Soc. 135 (2013) 610–612.
[48] J.A. Wiig, Y. Hu, C.C. Lee, M.W. Ribbe, Radical SAM-dependent carbon insertion into the nitrogenase M-cluster, Science 337 (2012) 1672–1675.
[49] E.R. Hall, C.J. Pollock, J. Bendix, T.J. Collins, P. Glatzel, S. DeBeer, Valence-to-core-detected X-ray absorption spectroscopy: targeting ligand selectivity, J. Am. Chem. Soc. 136 (2014) 10076–10084.
[50] Y.M. Xiao, K. Fisher, M.C. Smith, W.E. Newton, D.A. Case, S.J. George, H.X. Wang, W. Sturhahn, E.E. Alp, J.Y. Zhao, Y. Yoda, S.P. Cramer, How nitrogenase shakes — initial information about P-cluster and FeMo-cofactor normal modes from nuclear resonance vibrational spectroscopy (NRVS), J. Am. Chem. Soc. 128 (2006) 7608–7612.
[51] R. Bjornsson, M. Delgado, F. A. Lima, O. Einsle, F. Neese, S. DeBeer, Molybdenum L-Edge XAS Spectra of MoFe Nitrogenase Z. Anorg. Allg. Chem. (2014), http://dx.doi.org/10.1002/zaac.201400446.